



HAL
open science

Seasonal marine microorganisms change neighbours under contrasting environmental conditions

Stefan Lambert, Jean-claude Lozano, François-yves Bouget, Pierre E. Galand

► **To cite this version:**

Stefan Lambert, Jean-claude Lozano, François-yves Bouget, Pierre E. Galand. Seasonal marine microorganisms change neighbours under contrasting environmental conditions. *Environmental Microbiology*, 2021, 23, pp.2592 - 2604. 10.1111/1462-2920.15482 . hal-03830951

HAL Id: hal-03830951

<https://hal.science/hal-03830951v1>

Submitted on 28 Oct 2022

HAL is a multi-disciplinary open access archive for the deposit and dissemination of scientific research documents, whether they are published or not. The documents may come from teaching and research institutions in France or abroad, or from public or private research centers.

L'archive ouverte pluridisciplinaire **HAL**, est destinée au dépôt et à la diffusion de documents scientifiques de niveau recherche, publiés ou non, émanant des établissements d'enseignement et de recherche français ou étrangers, des laboratoires publics ou privés.

1 **Seasonal marine microorganisms change neighbors under contrasting**
2 **environmental conditions**

3

4 Stefan Lambert¹, Jean-Claude Lozano¹, François-Yves Bouget^{1,§} and Pierre E. Galand^{2,§}

5 ¹Sorbonne Université, CNRS, Laboratoire d'Océanographie Microbienne (LOMIC),
6 Observatoire Océanologique de Banyuls, Banyuls sur Mer, France.

7 ²Sorbonne Université, CNRS, Laboratoire d'Ecogéochimie des Environnements Benthiques
8 (LECOB), Observatoire Océanologique de Banyuls, Banyuls sur Mer, France.

9

10 [§] Corresponding authors

11 **Email:** pierre.galand@obs-banyuls.fr, francois-yves.bouget@obs-banyuls.fr

12

13

14

15

16

17

18

19

20

21 **Keywords :** picoeukaryotes, bacteria, archaea, time series, networks, perturbations, sola

22 **Author Contributions:** FYB and PEG designed research; SL and JCL performed research;

23 FYB, PEG and SL analyzed data; and FYB, PEG, SL wrote the paper.

24

25

26 **Originality-Significance Statement**

27 Planktonic microorganisms in the ocean play a key role for oxygen production, carbon
28 sequestration and nutrient recycling. These microbial functions are directly associated with
29 the composition of the communities, which changes regularly with seasons and shows strong
30 and reproducible patterns year after year. Remarkable weather events can dramatically
31 change the environment, but their effect on the stability of the microbial communities is not
32 known. Here we show that environmental perturbations transform and weaken the networks
33 of co-occurring eukaryotes, bacteria and archaea. In addition, individual taxa changed
34 neighbors from year to year, which could suggest switches between ecologically equivalent
35 microbes. Such unexpected unfaithful relationships between marine microorganisms may
36 promote the long term stability of the ecosystem.

37

38

39

40

41

42

43

44

45

46

47

48

49

50

51 **Summary**

52 Marine picoplankton contribute to global carbon sequestration and nutrient recycling. These
53 processes are directly related to the composition of communities, which in turn depends on
54 microbial interactions and environmental forcing. Under regular seasonal cycles, marine
55 communities show strong predictable patterns of annual re-occurrences, but little is known
56 about the effect of environmental perturbation on their organization. The aim of our study
57 was to investigate the co-occurrence patterns of planktonic picoeukaryote, bacteria and
58 archaea under contrasting environmental conditions. The study was designed to have high
59 sampling frequency that could match both the biological rhythm of marine microbes and the
60 short time scale of extreme weather events. Our results show that microbial networks
61 changed from year to year depending on conditions. In addition, individual taxa became less
62 interconnected and changed neighbors, which revealed an unfaithful relationship between
63 marine microorganisms. This unexpected pattern suggests possible switches between
64 organisms that have similar specific functions, or hints at the presence of organisms that
65 share similar environmental niches without interacting. Despite the observed annual changes,
66 the time series showed re-occurring communities that appear to recover from perturbations.
67 Changing co-occurrence patterns between marine microorganisms may allow the long-term
68 stability of ecosystems exposed to contrasting meteorological events.

69

70

71

72

73

74

75

76 **Introduction**

77 The global carbon and nutrient cycle in the surface waters of the ocean is strongly driven by
78 marine microbial communities (Falkowski et al., 2008). As microbial communities' function
79 and productivity are directly linked to community diversity and composition (Bell et al.,
80 2005), understanding patterns and processes of community assembly is crucial for the
81 prediction of ecosystem functioning (Nemergut et al., 2013). Microbial community assembly
82 is the outcome of biotic interactions such as competition, predation and mutualism, and
83 abiotic selection by local environmental conditions (Vellend, 2010; Nemergut et al., 2013). In
84 the ocean, there is a general consensus that microbial planktonic communities respond to the
85 physical chemical features of sea water. In temperate and polar regions, these features are
86 strongly associated with the seasonality of the ocean marked by changing temperature
87 regimes (Fuhrman et al., 2015). The dynamics of the ocean may be hard to capture by
88 discrete sampling schemes, and long-term oceanographic time-series studies have proven to
89 be very useful to elucidate links between microbial communities and environmental
90 conditions. Temperature, day length, photosynthetically available radiation, salinity and
91 nutrient concentrations are the main abiotic factors that individually or together strongly
92 impact the seasonal composition of microbial communities (e.g., (Treusch et al., 2009; Eiler
93 et al., 2011; Gilbert et al., 2012; Chow et al., 2013; Cram et al., 2015b; Salter et al., 2015;
94 Parada and Fuhrman, 2017; Auladell et al., 2019; Lambert et al., 2019)). Long term time-
95 series of microbial communities have also shown the importance of biotic forcing (Chow et
96 al., 2014; Ahlgren et al., 2019). Top-down controls, which include predation and viral lysis,
97 and bacteria–bacteria interactions are important factors that shape community assembly.
98 Microbial communities are complex systems of co-occurring species and the use of
99 interaction networks has strongly increased our understanding on the possible connections

100 between microorganisms within a community (Beman et al., 2011; Steele et al., 2011; Gilbert
101 et al., 2012; Chow et al., 2014; Cram et al., 2015a; Needham et al., 2017).

102 Time-series studies have demonstrated the strong predictability of microbial
103 community composition season after season, and year after year (Fuhrman et al., 2006). This
104 key feature has been seen repeatedly for bacteria and archaea (Hugoni et al., 2013; Chafee et
105 al., 2018; Galand et al., 2018), but also eukaryotes (Giner et al., 2019), and appears to be
106 maintained under irregular environmental perturbations (Lambert et al., 2019). This strong
107 pattern of re-occurrence has been explained by the invisible hand metaphor, which refers to
108 the cumulative effect of individuals working in their own self-interest that leads to well-
109 regulated community function without any centralized control mechanism (Fuhrman et al.,
110 2015). This long-term pattern has been observed at monthly sampling frequencies and the
111 question remains as to whether such a motif could be seen at higher sampling frequency.
112 Generation times of phytoplankton and marine bacteria can vary a lot, but are estimated to
113 range from a few hours to a few days (Kirchman, 2016). Daily or twice a week sampling
114 would thus better match the biological rhythm of the microbial sea (Fuhrman et al., 2015).

115 Higher frequency time-series studies have recently emerged and showed the rapid
116 transitions between closely related strains (Needham and Fuhrman, 2016; Ward et al., 2017;
117 Martin-Platero et al., 2018) and recurrent patterns of microdiversity in a coastal ecosystem
118 (Chafee et al., 2018). They have followed the succession of species during blooms over a few
119 months at a daily frequency (Needham and Fuhrman, 2016; Martin-Platero et al., 2018;
120 Needham et al., 2018) or twice a week (Teeling et al., 2012). Only a few have monitored the
121 dynamics of communities over longer time period: one year at a twice a week frequency
122 (Lindh et al., 2015) or 3 years at weekly/twice a week frequency (Ward et al., 2017; Chafee
123 et al., 2018). These studies have focused on prokaryotes and information on the long-term

124 high frequency dynamics of the 3 domains of life is lacking, and especially for coastal
125 ecosystems.

126 Temperate coastal ecosystems are impacted by land and particularly in the
127 Mediterranean Sea, where sudden and irregular weather events, such as strong precipitations
128 causing flash flooding, storms triggering sediment resuspension, or wind inducing water
129 column mixing, can have a strong impact (Charles et al., 2005; Thyssen et al., 2014; Tinta et
130 al., 2015). These contrasting weather conditions are predicted to increase with a changing
131 climate (Scoccimarro et al., 2016). The question remains as to whether community
132 successions, and interactions between marine microorganisms, can remain stable under
133 irregular climate events, or if the predicted increases in temperature and strong precipitations
134 could disrupt individual interactions within communities (Berner et al., 2018).

135 The aim of our study was to investigate the patterns of planktonic picoeukaryote,
136 bacteria and archaea co-occurrences under contrasting environmental conditions. The study
137 was designed to have a sampling frequency that could match both the biological rhythm of
138 marine microbes and the short time scale of extreme events such as flooding and storms.
139 Furthermore, the multiyear sampling was intended to discriminate recurrent microbial
140 community dynamics from stochastic events. We sampled the Banyuls Bay microbial
141 observatory (SOLA), a coastal site of the NW Mediterranean Sea, twice a week during the
142 most productive winter months (January-March) and weekly the rest of the time. Samples in
143 this study included those collected during an “average” year, with physical and chemical
144 parameters close to the long term mean, and two years marked by environmental winter
145 perturbations in terms of seawater temperature and freshwater influx.

146

147 **Results**

148 **Overall community composition, diversity and environmental conditions**

149 A canonical correspondence analysis (CCA) was carried out to compare the composition of
150 communities during the 3 high frequency sampling winter periods for the prokaryote (Fig.
151 1A) and eukaryote (Fig. 1B). Communities grouped generally by month of sampling but there
152 were some exceptions for both eukaryotes and prokaryotes, in particular samples from
153 December 2016, February 2017 and March 2017 were separated from the others for both
154 domains of life.

155 In order to precisely identify dissimilarities in community composition, we compared
156 systematically differences between successive samples (i.e. t sample vs t_{+1} sample) for the 3
157 winter periods (Supplementary Fig. 1). The most important dissimilarities were identified as
158 values above the annual average. They indicate abrupt changes in community composition
159 within a short period of time. Their occurrence was indicated by arrows on top of the
160 environmental conditions (Fig. 1C), and squares around CCA markers (Fig. 1A and B).
161 Seven out of the ten highest dissimilarities in community composition occurred in 2017.

162 During the winter season, which is the most productive time of the year at the site
163 {Galand, 2015 #2028}, the strong changes in community composition, marked by arrows,
164 corresponded most of the time to changes in salinity, but not always (Fig. 1C). These changes
165 were associated with increased nitrate concentrations and often to higher river discharge (Fig.
166 1C). This was clearly visible in March 2015 (red arrow), December 2016 (blue arrow),
167 February 2017 (blue arrow) and March 2017 (blue arrow).

168 The abrupt changes did not, however, impact the annual seasonality of the microbial
169 communities, which was characterized by repeatable temporal patterns in the community
170 composition, as shown by the higher similarity observed between communities sampled one
171 year apart and lower similarity for communities taken 6 months apart for both eukaryotes and
172 prokaryotes (Supplementary Fig. 2).

173 The Shannon diversity index pattern varied from year to year. Its range of variation
174 was low in 2015, decreased from January to April in 2016, and it was highly variable in 2017
175 (Supplementary Fig. 3).

176

177

178 **Community composition at the class level**

179 Among all the eukaryotic classes found in the dataset, four main classes dominated:
180 *Bacillariophyta*, *Dinophyceae*, *Mamiellophyceae* and *Syndiniales* (Supplementary Fig. 4).

181 Overall, for a given month, the average sequence abundance of these major groups varied
182 from year to year (Fig. 2). *Bacillariophyta*, which showed relatively low levels of average
183 sequence abundance throughout the sampling period, were more abundant in February and
184 March 2017. *Bacillariophyta* were almost absent in March 2016. Average abundance of
185 *Dinophyceae* remained relatively stable during the three years of sampling, with higher levels
186 in January and February 2017. *Mamiellophyceae* had more variable patterns of abundance. In
187 2015, they were more abundant in January and February, in 2016 they were more abundant in
188 March, and in 2017 in January. *Mamiellophyceae* were mainly composed of the genera
189 *Bathycoccus* and *Micromonas*. These two picoeukaryotes had different dynamics
190 characterized by a *Micromonas* bloom in early winter followed by *Bathycoccus* (ASV5 vs
191 ASV 4, Supplementary Fig. 5). *Syndiniales* abundance did not vary much in 2015, unlike in
192 2016 and 2017 when they were more abundant in March, and January/March respectively.

193 For prokaryotes, abundance of the main classes also varied from year to year and
194 especially in 2017 (Fig. 2). For *Alphaproteobacteria* decreases in abundance were seen in
195 February and March 2017. *Cyanobacteria* average abundances were relatively low and stable
196 during the three years of sampling, except for an increase in March 2017. Average abundance
197 for *Flavobacteria* in 2015 and 2016 showed an increase in March for both years.

198 *Flavobacteria*, in contrast, had a higher than average relative abundance in February 2017.
199 Finally, *Gammaproteobacteria* had similar levels of abundance between years from January
200 to March, except for February 2017 when they were less abundant (Fig. 2).

201

202

203 **Co-occurrence networks**

204 The co-occurrences of ASVs was investigated for each high frequency sampling winter
205 seasons (January, February and March) by network analysis based on the Maximal
206 Information Coefficient (MIC). MIC identifies correlations between variables and is best
207 adapted to the non-linear temporal nature of the data (Reshef et al., 2011). The networks,
208 based on significant MIC values ($p > 0.05$) with a false discovery rate (FDR) of 5%, show that
209 there were clear differences in the topology between years (Fig. 3). The 2015 network was
210 narrower, more clustered and more centralized than the 2016 and 2017 networks
211 (Supplementary Table 3).

212 The 2015 network was composed of 2 main modules, with a modularity of 12.4 and
213 5.7, respectively, as well as 4 smaller modules (modularity < 1) (Supplementary Table 4). The
214 ASVs that were more abundant in January and February grouped in one module (Fig. 3A). In
215 January, the hub ASVs defined as the nodes with highest degree, belonged first to
216 *Euryarchaeota* Marine Group II (Archaea), and then a number of Eukaryotes including
217 *Syndiniales*, diatoms (*Chaetoceros brevis*), a flagellate (*Florenciella parvula*) and
218 *Micromonas* (Mamiellophyceae) (Supplementary Table 5, Fig 3A). The hub ASVs of
219 February belonged to *Acidimicrobiales* (OM1 clade), *Gammaproteobacteria* clades ZD0405
220 and SAR86, and diatoms (*Chaetoceros curvisetus*). The second main module was composed
221 of ASVs abundant in March and included SAR11 surface 1 clade (*Alphaproteobacteria*),
222 *Flavobacteriales*, *Rhodobacteraceae* and *Syndiniales* (Eukaryota) as hubs. The 2015 network

223 did not show any discernible pattern with respect to temperature or salinity, but the highest
224 values were associated with the January ASVs (Fig. 3B, 3C).

225 The 2016 network consisted of 3 modules with a modularity of 14.5, 6 and 3,
226 respectively and followed a seasonal pattern, but with a distinct March module (Fig. 3A,
227 Supplementary Table 4). In January, the hub ASVs belonged to the cyanobacteria
228 *Prochlorococcus*, *Acidimicrobiales* OM1 clade, *Deltaproteobacteria* SAR324 clade, the
229 SAR11 surface 2 clade (*Alphaproteobacteria*) and to the dinoflagellate *Gymnodiniales*. In the
230 February group, the hubs were diatoms from the *Florenciellales* and Raphid-pennate
231 families, *Flavobacteriales* of the NS9 marine group and *Syndiniales*. The second module
232 contained ASVs that were more abundant in March. The hub ASVs were members of the
233 *Flavobacteriaceae*, MAST 6 (Stramenopiles), and *Syndiniales* (Supplementary Table 5).
234 *Micromonas* (*Mamiellophyceae*) was connected with both modules (Fig. 3). The 2016
235 network was separated into a low temperature (11-12°C) and a high temperature (13-14°C)
236 module (Fig. 3B), and the ASVs were mainly related to samples with higher salinity (38)
237 (Fig. 3C).

238 The 2017 network formed 8 low modularity modules (modularity between 4.4 and
239 0.5) (Fig. 3, Supplementary Table 4). A seasonal pattern within the ASVs was not as clear as
240 in 2015 and 2016. In January, abundant hub ASVs belonged to *Micromonas*
241 (*Mamiellophyceae*), *Thaumarchaeota* Marine group I (Archaea) and the flagellate algae
242 *Pelagomonas* (Supplementary Table 5). The ASVs abundant in February were separated in 2
243 groups. On the top of the network (Fig. 3A), diatoms (*Skeletonema*) were abundant, and the
244 hubs belonged to *Flavobacteriales* and, among Eukaryotes, *Lauderia* diatoms and the
245 phagotrophic flagellate *Ebria* (Cercozoa). In the second part of the network containing ASVs
246 abundant in February, a *Syndiniales* was abundant. The ASVs that were abundant in March
247 were in the middle of the network and the hubs were identified as *Synechococcus*

248 cyanobacteria, *Flavobacteriaceae* and the flagellate *Chrysochromulinaceae*. The 2017
249 network showed a central module with higher temperature (13°C), surrounded by lower
250 temperature modules (12°C) (Fig 3B). It was composed of modules of ASVs found under
251 average salinity of 37, and one module of low salinity ASVs (35) (Fig. 3C).

252

253

254

255 **ASV co-occurrences**

256 In the networks, a total of 42 ASVs were common to the three high frequency winter
257 samplings (Supplementary Fig. 6). In order to assess if the first neighbor nodes of the 42
258 common ASVs changed from year to year, we represented the positive co-occurrences in
259 radar plots (Fig. 4). The radius of the spider net corresponds to the MIC score between the
260 central ASV and its first neighbors.

261 Noteworthy, all of the 42 ASVs changed neighbors between years. The number of
262 first neighbors also changed from year to year (Fig. 4, Supplementary Table 6). Overall, the
263 total number of first neighbors decreases from 2015 to 2017 (542, 389 and 263 in 2015, 2016
264 and 2017 respectively). Half of the ASV (21) had a larger number of first neighbors in 2015
265 compared to the other years. A total of 16 ASVs had more first neighbors in 2016 and only 2
266 had more neighbors in 2017. Three ASVs had years with similar number of neighbors (Fig.
267 4). The total number of neighbors per year varied greatly between ASVs. The highest values
268 were 51 for ASV38 (*Alphaproteobacteria*) and the lowest 6 for ASV10 (*Flavobacteria*) (Fig.
269 4, Supplementary Table 6).

270 Among the common ASVs, 23 were earlier identified as rhythmic over 7 years
271 (Lambert et al., 2019) (marked by a black frame, Fig. 4). They also had first neighbors that
272 varied in number and identity between years (Fig. 4). Finally, bacterial ASVs were mostly

273 associated with bacteria (59% of the first neighbors) while eukaryotic ASVs were mostly
274 associated with eukaryotes (67% of the first neighbors). However, the affiliation of the first
275 neighbor to a given domain of life also changed from year to year. For a given ASV, some
276 years showed more eukaryotic first neighbors while other displayed more prokaryotic
277 neighbors.

278

279

280 **Discussion**

281 Our high frequency sampling study, focusing on the productive winter months, showed that
282 the patterns of the microbial networks linking members of the 3 domains of life changed from
283 year to year. To the best of our knowledge, inter-annual variations of network topology have
284 not been shown earlier. On the contrary, a recent high frequency sampling study from the
285 North Sea reported that network topologies were similar for co-varying microbes between
286 two different years for a same season (Chafee et al., 2018). Networks have, however, been
287 shown to change between seasons in both freshwater (Kara et al., 2013; Hu et al., 2017) and
288 marine environments (Chafee et al., 2018; Cui et al., 2019). Different temporal patterns in
289 network topology have also been observed along shorter time series (Martin-Platero et al.,
290 2018). These temporal changes reflect variations in community composition with changing
291 environmental conditions along a year (Fuhrman et al., 2015). Nevertheless, these earlier
292 studies did not test the year to year stability of the networks. Many correlation-based
293 association networks have focused only on the overall trend of microbial interconnectivity
294 without distinguishing seasons and years, the goal being to identify time-dependent
295 associations among ecologically important taxa (Steele et al., 2011; Chow et al., 2013;
296 Needham et al., 2013; Chow et al., 2014; Cram et al., 2015a; Milici et al., 2016; Needham et

297 al., 2017; Parada and Fuhrman, 2017). The fact that network topologies can change from year
298 to year should be considered in future temporal studies.

299 The long-term stability of co-occurrences has not been tested earlier. Co-occurrences
300 could have been considered to be robust and maintained over time since similar microbial
301 communities have been shown to reoccur, at a same site, year after year (Fuhrman et al.,
302 2006; Gilbert et al., 2012; Lambert et al., 2019). We also observed annual patterns of
303 reoccurrence, but our data revealed that despite these reproducible patterns, the microbial
304 networks are not necessarily robust as their topology can be broken when climatic conditions
305 changes.

306 Interestingly, the abrupt or gradual changes (salinity and temperature) that we
307 observed did not impact the overall rhythmicity of the microbial sea over the long term
308 (Lambert et al., 2019) nor in this study. Regardless of the environmental perturbations, some
309 ASVs reoccur every year. However, here we observed that these reoccurring ASVs rarely had
310 the same first neighbors, which indicate very strong changes of co-occurrence patterns from
311 year to year. The changing patterns probably correspond to the changing environmental
312 conditions that included higher sea water temperature in 2015-2016 and numerous salinity
313 drops in 2016-2017. Strong changes were also seen in the overall number of first neighbors
314 within a network, which was halved from 2015 to 2017. Nodes with fewer neighbors may be
315 an indication of a less robust network (Röttjers and Faust, 2018) and may thus illustrate a
316 possible weakening of the network of co-occurrence by environmental perturbations.

317 The observed changes in co-occurrence patterns may have different explanations.
318 First, if we hypothesize that co-occurrences represent interactions between microorganisms,
319 such as cross feeding, predation or parasitism (Fuhrman et al., 2015), it could mean that some
320 species might be replaced by others having a similar function. It could be the case for
321 *Micromonas* (ASV5) that co-occurred with different potential ciliate predators between 2015

322 and 2017. The possibility for a partial functional redundancy at the individual level has been
323 described earlier (Galand et al., 2018). Although there may not be functional redundancy at
324 the community level (Galand et al., 2018), at the individual level, a switch between different
325 organisms that have a same specific function is possible. In our study, a gene level functional
326 redundancy may exist for the *Rhodobacterales* and the *Oceanospirillales*, or the
327 *Thaumarchaeota*, which all could produce B12 (Doxey et al., 2015; Gómez-Consarnau et al.,
328 2018), and that change co-occurrences with the *Mamiellophyceae* that are B12 auxotrophs
329 (*Bathycoccus* ASV_euk4, *Micromonas* ASV_euk22). Our study is, however, focused on the
330 small size fraction of the microbial communities and thus misses larger planktonic organisms.
331 Phytoplankton is known to interact with prokaryotes, but these interactions, and their possible
332 stability over time, cannot be accounted for in our analysis.

333 The other hypothesis for the change of neighbors is that there are only limited
334 interactions between species, and that the co-occurrence patterns only represent species
335 having preferences for similar environmental conditions, i.e they share similar niches. This
336 would imply that the strong seasonal patterns, such as the ones observed for dominant ASVs
337 like *Mamiellophyceae* or SAR11, would be driven by structuring environmental parameters
338 like temperature and day length (Gilbert et al., 2012; Lambert et al., 2019). The reality
339 probably reflects a mix of both hypotheses with the presence of microorganisms that are
340 unfaithful in their interactions, and cohorts that respond to similar environmental conditions.

341 The abrupt perturbations that we observed at the Banyuls microbial observatory
342 (SOLA) were characterized by lower sea water salinity. These drops corresponded to
343 episodes of heavy rain leading to higher water level in the local river. Large rivers further up
344 the coast have also been shown to impact the study site (Laghdass et al., 2010). Episodes of
345 heavy rain are often concomitant with storms in the North Eastern Mediterranean (Charles et
346 al., 2005; Guizien et al., 2007). Storms mix the sea floor sediments through the water column,

347 which increases nutrient concentrations. Nutrients are also brought from land by the river and
348 can induce blooms measured as peak of chlorophyll, as seen earlier along the coast of the
349 eastern Mediterranean (Charles et al., 2005; Nunes et al., 2018).

350 At the Banyuls site, the strongest low salinity events were observed during winter 2016-2017.
351 The perturbations resulted in lower relative abundance of the predominant marine bacteria
352 SAR11 (*Alphaproteobacteria*) and an increase of *Flavobacteria*. Among picoeukaryotes, the
353 parasitic *Syndiniales* increased in relative abundance. The corresponding microbial network
354 was characterized by a low salinity module that was composed of diatoms of the genus
355 *Skeletonema* and *Lauderia*, and highly connected bacteria of the family *Flavobacteriaceae*
356 and *Rhodobacteraceae*. Our results suggest that the freshwater input, and the associated
357 nutrients, favored the bloom of specific diatoms species that were co-occurring with bacteria
358 that are usually not abundant in the Bay of Banyuls at that time of the year. These bacteria
359 have been seen associated with diatom blooms earlier (Teeling et al., 2016), and diatoms
360 have been shown to bloom following episodic fertilization events associated with freshwater
361 runoff (Tinta et al., 2015; Nunes et al., 2018). *Skeletonema* in particular was observed to
362 bloom following heavy rains along the Catalan coast (Estrada, 1979). It should, however, be
363 noted that microorganisms like diatoms are not expected to pass through our 3 μm filters. The
364 fact that we detected sequences from larger cells suggests that DNA from damaged or lysed
365 organisms passed through the pre-filter. The interpretation of the co-occurrence patterns is
366 thus done within the frame of this technical limitation.

367 Winter 2015-2016 was characterized by higher sea water temperatures in January and
368 February compared to average. These higher temperatures may have impacted the bloom of
369 *Micromonas* that took place later that year compared to average (February instead of
370 January). They may have been replaced by Cyanobacteria (*Prochlorococcus*) that increased
371 in sequence abundance and became hub species in the network in January. *Prochlorococcus*

372 are overall less abundant than *Synechococcus* in the NW Mediterranean Sea (Schauer et al.,
373 2003), but appear to bloom in autumn when solar radiations are weaker (Sommaruga et al.,
374 2005). Our results suggest that when sea water temperature remains relatively high in early
375 winter, the bloom of *Prochlorococcus* can persist at the expense of *Micromonas*
376 development. Such a switch could have an impact on the functioning of the coastal NW
377 Mediterranean. It has, for example, been shown that after a mild winter in the Baltic Sea the
378 spring bloom was reduced, thus impacting the carbon cycle (Legrand et al., 2015). Such a
379 scenario could lead to lower carbon export to the marine food web (Berner et al., 2018).

380 Winter 2014-2015 had environmental conditions that were the most similar to an
381 average year. The corresponding microbial network was marked by a clear separation
382 between seasonal modules. It corresponded to the temporal succession of species in the
383 coastal NW Mediterranean, which is marked by a strong seasonality (Hugoni et al., 2013;
384 Galand et al., 2018; Lambert et al., 2019). In January, the hub species were picoeukaryotes
385 identified as *Micromonas* (class *Mamiellophyceae*), *Euryarchaeota* Marine Group II
386 (*Archaea*), and diatoms (*Chaetoceros brevis*). A *Micromonas* bloom at the beginning of the
387 year has been seen earlier at the Banyuls site (Lambert et al., 2019), but its co-occurrence
388 with *Euryarchaeota* has not been reported. In February, the communities were characterized
389 by diatoms of the genus *Chaetoceros* and bacteria belonging to the ZD0405 and SAR86
390 clades of *Gammaproteobacteria*. These bacteria have been reported as associated with
391 diatom blooms earlier (Lucas et al., 2015; Teeling et al., 2016). In March, the hub species
392 corresponded to classical pelagic microbial communities composed of the SAR11 surface 1
393 clade (*Alphaproteobacteria*) and *Bathycoccus* for the pico-eukaryotes, which is known to
394 bloom in late winter at the site (Lambert et al., 2019). As *Bathycoccus* and SAR11 are both
395 auxotroph to vitamin B1 precursors, their co-occurrence may reflect shared ecological niches

396 rather than interaction as proposed for co-occurring *Micromonas* and SAR11 (Lambert et al.,
397 2019).

398

399 **Conclusions**

400 Our high frequency sampling of NW Mediterranean microbial communities revealed that co-
401 occurrence networks of picoeukaryote, bacteria and archaea changed from year to year.
402 Weather perturbations in temperature or salinity seem to alter the topology of the microbial
403 networks. In addition, individual taxa changed neighbor from year to year suggesting an
404 unfaithful relationship between marine microorganisms. However, the global seasonal
405 patterns of rhythmic ASVs were maintained, which indicates that the communities recover
406 from these perturbations. It implies a strong environmental control, but it also suggests that
407 changing co-occurrences between marine microorganisms may allow the long-term stability
408 of the ecosystem. The resilience of seasonal microbial ecosystems remains, however, to be
409 assessed under the more extreme climatic events predicted for the future. Well-established
410 time series are essential for the monitoring of anthropological impacts on the sea and to get a
411 good understanding of the functioning of the microbial ocean.

412

413 **Experimental Procedures**

414

415 **Sampling**

416 Surface water (3m) was collected with Niskin bottles from January 2015 to March 2017 at
417 the Banyuls Bay microbial observatory (SOLA) (42°31'N, 03°11'E) in the Bay of Banyuls-
418 sur-Mer, North Western Mediterranean Sea, France. A total of 5 L of seawater was
419 prefiltered through 3 µm pore-size polycarbonate filters (Merck-Millipore, Darmstadt,
420 Germany), and the microbial biomass was collected on 0.22-µm pore-size GV Sterivex

421 cartridges (Merck-Millipore) and stored at -80 °C until nucleic acid extraction. Samples were
422 collected twice a week during winters: January to March 2015, January to April 2016 and
423 December 2016 to March 2017, and once a week otherwise (spring, summer and autumn).
424 The physicochemical (temperature, salinity, day length, nitrate, nitrite, silicate and phosphate
425 concentrations) and biological (chlorophyll a) were provided by the Service d'Observation en
426 Milieu Littoral (SOMLIT). The levels of the river discharging in the bay of Banyuls, the
427 Baillaury, were obtained from the “Service Central d'Hydrométéorologie et d'Appui à la
428 Prévision des Inondations” (<http://www.hydro.eaufrance.fr/>).

429

430 **DNA extraction, amplification and sequencing**

431 The nucleic acid extraction followed protocols published earlier (Lambert et al., 2019). To
432 summarize, the Sterivex filters were thawed on ice, followed by addition of lysis buffer
433 (40nM EDTA, 50nM Tris, 0.75M sucrose) and 25 µL of lysozyme (20 mg mL⁻¹). The filters
434 were then incubated for 45 minutes at 37°C on a rotary mixer. Subsequently, 8µL of
435 Proteinase K (20mg mL⁻¹) and 26µL of sodium dodecyl sulfate (20% v/v) were added before
436 incubating for 1 hour at 55°C. Total DNA was then extracted and purified with the Qiagen
437 AllPrep kit (Qiagen, Hilden, Germany) following the kit's protocol.

438 Specific primers were used to target the eukaryotic V4 region (TAReuk_F1 [5'-
439 CCAGCASCYGC GGTAATTCC] and TAReuk_R [5'-ACTTTCGTTCTTGATYRATGA],
440 (Stoeck et al., 2010) and the prokaryotic V4-V5 region (515F-Y [5'-
441 GTGYCAGCMGCCGCGGTAA] and 926R [5'-CCGYCAATTYMTTTRAGTTT] (Parada
442 et al., 2016). Library preparation and sequencing were carried out by the Genotoul platform
443 (Toulouse, France), with the Illumina Miseq 2x250 bp kits. All sequences were deposited in
444 NCBI under accession number PRJNA579489.

445

446 **Sequence analysis and preprocessing**

447 The standard pipeline of the DADA2 package (v1.6) (Callahan et al., 2016) in “R” was used
448 to do the analysis of the raw sequences. The parameters used for the eukaryote dataset were:
449 trimLeft=c(20, 21) ,truncLen=c(250,250), maxN=0, maxEE=c(2,2), truncQ=2; and for the
450 prokaryote dataset: trimLeft=c(19, 20), truncLen=c(240,200), maxN=0, maxEE=c(2,5),
451 truncQ=2. We analyzed 141 and 142 samples for the eukaryote and prokaryote datasets
452 respectively, and obtained a total of 3.8 and 3.4 million reads respectively after DADA2 data
453 processing (Supplementary Table 1). The taxonomy assignment was done with the The
454 Protist Ribosomal Reference database (PR²)v.4.10.0 (Guillou et al., 2012) database for the
455 eukaryotes and with SILVA v.128 database (Quast et al., 2013) for the prokaryote. The
456 “assignTaxonomy” function in DADA2 implements the RDP naive Bayesian classifier
457 method (Wang et al., 2007).

458 Taxa belonging to the supergroup “Opisthokonta” were removed from the eukaryote
459 dataset and taxa belonging to eukaryotes were removed from the prokaryote dataset. Samples
460 containing less than 5000 reads and 9000 reads were removed from the eukaryote and
461 prokaryote dataset respectively. A total of 139 and 137 samples remained for the eukaryotes
462 and the prokaryotes respectively. These preprocessing steps were done with the “R” package
463 “Phyloseq” (McMurdie and Holmes, 2013).

464 Microbial communities in this study and in our previous study (Lambert et al., 2019)
465 were not amplified with the same primer set. Here we chose to use universal primers shown
466 to have a good coverage of both Bacteria and Archaea (Parada et al., 2016) instead of the
467 two sets of separate primers used earlier (Lambert et al., 2019). In order to identify in this
468 study the ASVs that were detected as rhythmic in our previous study, we compared both
469 datasets by BLAST (Altschul et al., 1997) (blastn, >99% identity). For the eukaryotes, reads
470 from both studies overlapped (~230 bp), and we could thus do a direct identification

471 (Supplementary Table 2). For the prokaryotes, however, the reads did not have an
472 overlapping region. We therefore did a first BLAST of the rhythmic prokaryotic ASVs
473 (Lambert et al., 2019) against the SILVA v.128 database. The matching sequences were then
474 extracted from SILVA to create a novel custom database. Finally, we did a BLAST of the
475 prokaryotic ASVs from this study against the custom database (Supplementary Table 2). We
476 could then identify the ASVs from Lambert et al 2019 and the ASVs from this study that
477 exactly matched the same SILVA reference sequence.

478

479 **Statistics**

480 Sequence counts for both datasets were normalized with the median-ratio method
481 implemented in the “DESeq2” package (Love et al., 2014), which is mathematically
482 equivalent to the compositional log-ratio (clr) transformation that accounts for the
483 compositional nature of the data (Quinn et al., 2018).

484 The Bray-Curtis dissimilarity index was calculated with the “vegdist” function of the
485 “Vegan” package (Oksanen et al., 2019) in “R”. Distances between samples were calculated
486 based on community composition with a canonical correspondence analyses (CCA) with the
487 “Vegan” package in "R". Contribution of environmental factors were added as arrows.

488 Abrupt changes in community composition between two samples were identified as
489 Bray-Curtis dissimilarity values peaking above average. For that purpose, the Bray-Curtis
490 dissimilarity index was calculated between two successive samples (t vs t_{+1}), within each
491 dataset, to identify variations of community composition with time.

492 Networks were based on the Maximal Information Coefficient (MIC), a measure that
493 effectively identifies relationships between variables and that is best adapted to the non-linear
494 temporal nature of the data, and behave well with small datasets (Reshef et al., 2011). The
495 MIC was computed for each year based on ASV tables containing the most abundant ASVs.

496 They were selected as the 20 most abundant ASVs per sample, in each dataset, over each
497 winter period (January, February, March), and represented over all a total of 153 ASVs in
498 2015, 182 in 2016 and 187 in 2017. The MIC was then used to build a network that was
499 visualized in Cytoscape (Shannon et al., 2003). The full network was pruned to visualize
500 ASV interactions that had a Pearson linear regression > 0 (positive interactions) and a MIC $>$
501 0.75 . These MIC values corresponded to significant interactions ($p < 0.05$) when accepting a
502 false discovery rate (FDR) of 5% at most as computed with MICtools (Albanese et al., 2018).
503 The layout chosen for the network was edge-weighted spring embedded, using the MIC
504 parameter. Module analyses were done with the CytoCluster app (Li et al., 2017) for
505 Cytoscape, using the HC-PIN clustering algorithm with the default parameters (Weak,
506 Threshold: 2.0 and ComplexSize Threshold: 3). Network analysis was done using the
507 NetworkAnalyzer tool included in Cytoscape. Hub ASVs, which are the ones associated with
508 a high number of other ASVs, were defined for each network as the nodes with highest
509 degree (Röttjers and Faust, 2018). The networks were treated as undirected.

510 Radar plots were made with the "fmsb" package ([https://cran.r-](https://cran.r-project.org/web/packages/fmsb)
511 [project.org/web/packages/fmsb](https://cran.r-project.org/web/packages/fmsb)) in "R". The heatmap was made with the "Phyloseq"
512 package. For this figure, the eukaryotic and prokaryotic datasets were merged. Only ASVs
513 with more than 10 reads were represented.

514

515 **Acknowledgments**

516 We are grateful to the captain and the crew of the RV 'Nereis II' for their help in acquiring
517 the samples. We thank the "Service d'Observation", particularly Eric Maria and Paul Labatut,
518 for their help in obtaining and processing of the samples. SL was supported by a PhD
519 fellowship from the doctoral school ED129. This work was supported by the French Agence

520 Nationale de la Recherche through the projects Photo-Phyto (ANR-14-CE02-0018) to FYB,
521 and EUREKA
522 (ANR-14-CE02-0004-01) to PEG.

523

524 **References:**

- 525 Ahlgren, N.A., Perelman, J.N., Yeh, Y.C., and Fuhrman, J.A. (2019) Multi-year dynamics of
526 fine-scale marine cyanobacterial populations are more strongly explained by phage
527 interactions than abiotic, bottom-up factors. *Environ Microbiol* 21: 2948-2963.
- 528 Albanese, D., Riccadonna, S., Donati, C., and Franceschi, P. (2018) A practical tool for
529 maximal information coefficient analysis. *GigaScience* 7: 1-8.
- 530 Altschul, S.F., Madden, T.L., Schaffer, A.A., Zhang, J., Zhang, Z., and Miller, W. (1997)
531 Gapped BLAST and PSI-BLAST: a new generation of protein database search programs.
532 *Nucleic Acids Res* 25: 3389-3402.
- 533 Auladell, A., Sánchez, P., Sánchez, O., Gasol, J.M., and Ferrera, I. (2019) Long-term
534 seasonal and interannual variability of marine aerobic anoxygenic photoheterotrophic
535 bacteria. *ISME J*: 1.
- 536 Bell, T., Newman, J.A., Silverman, B.W., Turner, S.L., and Lilley, A.K. (2005) The
537 contribution of species richness and composition to bacterial services. *Nature* 436: 1157-
538 1160.
- 539 Beman, J.M., Steele, J.A., and Fuhrman, J.A. (2011) Co-occurrence patterns for abundant
540 marine archaeal and bacterial lineages in the deep chlorophyll maximum of coastal
541 California. *ISME J* 5: 1077.
- 542 Berner, C., Bertos-Fortis, M., Pinhassi, J., and Legrand, C. (2018) Response of Microbial
543 Communities to Changing Climate Conditions During Summer Cyanobacterial Blooms in the
544 Baltic Sea. *Front Microbiol* 9: 1562.
- 545 Callahan, B.J., McMurdie, P.J., Rosen, M.J., Han, A.W., Johnson, A.J.A., and Holmes, S.P.
546 (2016) DADA2: high-resolution sample inference from Illumina amplicon data. *Nat Methods*
547 13: 581.
- 548 Chafee, M., Fernández-Guerra, A., Buttigieg, P.L., Gerdt, G., Eren, A.M., Teeling, H., and
549 Amann, R.L. (2018) Recurrent patterns of microdiversity in a temperate coastal marine
550 environment. *ISME J* 12: 237.
- 551 Charles, F., Lantoin, F., Brugel, S., Chrétiennot-Dinet, M.-J., Quiroga, I., and Rivière, B.
552 (2005) Seasonal survey of the phytoplankton biomass, composition and production in a
553 littoral NW Mediterranean site, with special emphasis on the picoplanktonic contribution.
554 *Estuar Coast Shelf Sci* 65: 199-212.
- 555 Chow, C.-E.T., Kim, D.Y., Sachdeva, R., Caron, D.A., and Fuhrman, J.A. (2014) Top-down
556 controls on bacterial community structure: microbial network analysis of bacteria, T4-like
557 viruses and protists. *ISME J* 8: 816.
- 558 Chow, C.-E.T., Sachdeva, R., Cram, J.A., Steele, J.A., Needham, D.M., Patel, A. et al. (2013)
559 Temporal variability and coherence of euphotic zone bacterial communities over a decade in
560 the Southern California Bight. *ISME J* 7: 2259-2273.
- 561 Cram, J.A., Xia, L.C., Needham, D.M., Sachdeva, R., Sun, F., and Fuhrman, J.A. (2015a)
562 Cross-depth analysis of marine bacterial networks suggests downward propagation of
563 temporal changes. *ISME J* 9: 2573.

564 Cram, J.A., Chow, C.-E.T., Sachdeva, R., Needham, D.M., Parada, A.E., Steele, J.A., and
565 Fuhrman, J.A. (2015b) Seasonal and interannual variability of the marine bacterioplankton
566 community throughout the water column over ten years. *ISME J* 9: 563.
567 Cui, Y., Chun, S.-J., Baek, S.H., Lee, M., Kim, Y., Lee, H.-G. et al. (2019) The water depth-
568 dependent co-occurrence patterns of marine bacteria in shallow and dynamic Southern Coast,
569 Korea. *Sci Rep* 9: 1-13.
570 Doxey, A.C., Kurtz, D.A., Lynch, M.D.J., Sauder, L.A., and Neufeld, J.D. (2015) Aquatic
571 metagenomes implicate Thaumarchaeota in global cobalamin production. *ISME J* 9: 461-471.
572 Eiler, A., Hayakawa, D.H., and Rappé, M.S. (2011) Non-random assembly of
573 bacterioplankton communities in the subtropical North Pacific Ocean. *Front Microbiol* 2:
574 140.
575 Estrada, M. (1979) Observaciones sobre la heterogeneidad del fitoplancton en una zona
576 costera del mar Catalán. *Inv Pesq* 43: 637-666.
577 Falkowski, P.G., Fenchel, T., and Delong, E.F. (2008) The microbial engines that drive
578 Earth's biogeochemical cycles. *Science* 320: 1034-1039.
579 Fuhrman, J.A., Cram, J.A., and Needham, D.M. (2015) Marine microbial community
580 dynamics and their ecological interpretation. *Nat Rev Micro* 13: 133-146.
581 Fuhrman, J.A., Hewson, I., Schwalbach, M.S., Steele, J.A., Brown, M.V., and Naeem, S.
582 (2006) Annually reoccurring bacterial communities are predictable from ocean conditions.
583 *Proc Natl Acad Sci USA* 103: 13104-13109.
584 Galand, P.E., Pereira, O., Hochart, C., Auguet, J.C., and Debroas, D. (2018) A strong link
585 between marine microbial community composition and function challenges the idea of
586 functional redundancy. *ISME J* 12: 2470.
587 Gilbert, J.A., Steele, J.A., Caporaso, J.G., Steinbrück, L., Reeder, J., Temperton, B. et al.
588 (2012) Defining seasonal marine microbial community dynamics. *ISME J* 6: 298-308.
589 Giner, C.R., Balagué, V., Krabberød, A.K., Ferrera, I., Reñé, A., Garcés, E. et al. (2019)
590 Quantifying long-term recurrence in planktonic microbial eukaryotes. *Mol Ecol* 28: 923-935.
591 Gómez-Consarnau, L., Sachdeva, R., Gifford, S.M., Cutter, L.S., Fuhrman, J.A.,
592 Sañudo-Wilhelmy, S.A., and Moran, M.A. (2018) Mosaic patterns of B-vitamin synthesis
593 and utilization in a natural marine microbial community. *Environ Microbiol* 20: 2809-2823.
594 Guillou, L., Bachar, D., Audic, S., Bass, D., Berney, C., Bittner, L. et al. (2012) The Protist
595 Ribosomal Reference database (PR2): a catalog of unicellular eukaryote Small Sub-Unit
596 rRNA sequences with curated taxonomy. *Nucleic Acids Res* 41: D597-D604.
597 Guizien, K., Charles, F., Lantoine, F., and Naudin, J.-J. (2007) Nearshore dynamics of
598 nutrients and chlorophyll during Mediterranean-type flash-floods. *Aquat Living Resour* 20:
599 3-14.
600 Hu, A., Ju, F., Hou, L., Li, J., Yang, X., Wang, H. et al. (2017) Strong impact of
601 anthropogenic contamination on the co-occurrence patterns of a riverine microbial
602 community. *Environ Microbiol* 19: 4993-5009.
603 Hugoni, M., Taib, N., Debroas, D., Domaizon, I., Jouan Dufournel, I., Bronner, G. et al.
604 (2013) Structure of the rare archaeal biosphere and seasonal dynamics of active ecotypes in
605 surface coastal waters. *Proc Natl Acad Sci USA* 110: 6004-6009.
606 Kara, E.L., Hanson, P.C., Hu, Y.H., Winslow, L., and McMahon, K.D. (2013) A decade of
607 seasonal dynamics and co-occurrences within freshwater bacterioplankton communities from
608 eutrophic Lake Mendota, WI, USA. *ISME J* 7: 680-684.
609 Kirchman, D.L. (2016) Growth rates of microbes in the oceans. *Annu Rev Mar Sci* 8: 285-
610 309.
611 Laghdass, M., West, N.J., Batailler, N., Caparros, J., Catala, P., Lantoine, F. et al. (2010)
612 Impact of lower salinity waters on bacterial heterotrophic production and community
613 structure in the offshore NW Mediterranean Sea. *Environ Microbiol Rep* 2: 761-769.

614 Lambert, S., Tragin, M., Lozano, J.-C., Ghiglione, J.-F., Vaultot, D., Bouget, F.-Y., and
615 Galand, P.E. (2019) Rhythmicity of coastal marine picoeukaryotes, bacteria and archaea
616 despite irregular environmental perturbations. *ISME J* 13: 388-401.

617 Legrand, C., Fridolfsson, E., Bertos-Fortis, M., Lindehoff, E., Larsson, P., Pinhassi, J., and
618 Andersson, A. (2015) Interannual variability of phyto-bacterioplankton biomass and
619 production in coastal and offshore waters of the Baltic Sea. *AMBIO* 44: 427-438.

620 Li, M., Li, D., Tang, Y., Wu, F., and Wang, J. (2017) CytoCluster: A cytoscape plugin for
621 cluster analysis and visualization of biological networks. *Int J Mol Sci* 18: 1880.

622 Lindh, M.V., Sjöstedt, J., Andersson, A.F., Baltar, F., Hugerth, L.W., Lundin, D. et al. (2015)
623 Disentangling seasonal bacterioplankton population dynamics by high-frequency sampling.
624 *Environ Microbiol* 17: 2459-2476.

625 Love, M.I., Huber, W., and Anders, S. (2014) Moderated estimation of fold change and
626 dispersion for RNA-seq data with DESeq2. *Genome Biol* 15: 550.

627 Lucas, J., Wichels, A., Teeling, H., Chafee, M., Scharfe, M., and Gerdtts, G. (2015) Annual
628 dynamics of North Sea bacterioplankton: seasonal variability superimposes short-term
629 variation. *FEMS Microbiol Ecol* 91: fiv099.

630 Martin-Platero, A.M., Cleary, B., Kauffman, K., Preheim, S.P., McGillicuddy, D.J., Alm,
631 E.J., and Polz, M.F. (2018) High resolution time series reveals cohesive but short-lived
632 communities in coastal plankton. *Nat Commun* 9: 266.

633 McMurdie, P.J., and Holmes, S. (2013) phyloseq: an R package for reproducible interactive
634 analysis and graphics of microbiome census data. *PloS one* 8: e61217.

635 Milici, M., Deng, Z.-L., Tomasch, J., Decelle, J., Wos-Oxley, M.L., Wang, H. et al. (2016)
636 Co-occurrence analysis of microbial taxa in the Atlantic Ocean reveals high connectivity in
637 the free-living bacterioplankton. *Front Microbiol* 7: 649.

638 Needham, D.M., and Fuhrman, J.A. (2016) Pronounced daily succession of phytoplankton,
639 archaea and bacteria following a spring bloom. *Nat Microbiol* 1: 16005.

640 Needham, D.M., Sachdeva, R., and Fuhrman, J.A. (2017) Ecological dynamics and co-
641 occurrence among marine phytoplankton, bacteria and myoviruses shows microdiversity
642 matters. *ISME J* 11: 1614.

643 Needham, D.M., Chow, C.-E.T., Cram, J.A., Sachdeva, R., Parada, A., and Fuhrman, J.A.
644 (2013) Short-term observations of marine bacterial and viral communities: patterns,
645 connections and resilience. *ISME J* 7: 1274-1285.

646 Needham, D.M., Fichot, E.B., Wang, E., Berdjeb, L., Cram, J.A., Fichot, C.G., and Fuhrman,
647 J.A. (2018) Dynamics and interactions of highly resolved marine plankton via automated
648 high-frequency sampling. *ISME J* 12: 2417.

649 Nemergut, D.R., Schmidt, S.K., Fukami, T., O'Neill, S.P., Bilinski, T.M., Stanish, L.F. et al.
650 (2013) Patterns and processes of microbial community assembly. *Microbiol Mol Biol Rev*
651 77: 342-356.

652 Nunes, S., Latasa, M., Gasol, J.M., and Estrada, M. (2018) Seasonal and interannual
653 variability of phytoplankton community structure in a Mediterranean coastal site. *Mar Ecol*
654 *Prog Ser* 592: 57-75.

655 Oksanen, J., Blanchet, F.G., Kindt, R., Legendre, P., Minchin, P.R., O'hara, R. et al. (2019)
656 Package 'vegan'. Community ecology package, version 2.5-6.

657 Parada, A.E., and Fuhrman, J.A. (2017) Marine archaeal dynamics and interactions with the
658 microbial community over 5 years from surface to seafloor. *ISME J* 11: 2510-2525.

659 Parada, A.E., Needham, D.M., and Fuhrman, J.A. (2016) Every base matters: assessing small
660 subunit rRNA primers for marine microbiomes with mock communities, time series and
661 global field samples. *Environ Microbiol* 18: 1403-1414.

662 Quast, C., Pruesse, E., Yilmaz, P., Gerken, J., Schweer, T., Yarza, P. et al. (2013) The
663 SILVA ribosomal RNA gene database project: improved data processing and web-based
664 tools. *Nucleic Acids Res* 41: D590-D596.

665 Quinn, T.P., Erb, I., Richardson, M.F., and Crowley, T.M. (2018) Understanding sequencing
666 data as compositions: an outlook and review. *Bioinformatics (Oxford, England)* 34: 2870-
667 2878.

668 Reshef, D.N., Reshef, Y.A., Finucane, H.K., Grossman, S.R., McVean, G., Turnbaugh, P.J. et
669 al. (2011) Detecting Novel Associations in Large Data Sets. *Science* 334: 1518-1524.

670 Röttjers, L., and Faust, K. (2018) From hairballs to hypotheses—biological insights from
671 microbial networks. *FEMS Microbiol Rev* 42: 761-780.

672 Salter, I., Galand, P.E., Fagervold, S.K., Lebaron, P., Obernosterer, I., Oliver, M.J. et al.
673 (2015) Seasonal dynamics of active SAR11 ecotypes in the oligotrophic Northwest
674 Mediterranean Sea. *ISME J* 9: 347-360.

675 Schauer, M., Balagué, V., Pedrós-Alió, C., and Massana, R. (2003) Seasonal changes in the
676 taxonomic composition of bacterioplankton in a coastal oligotrophic system. *Aquat Microb
677 Ecol* 31: 163-174.

678 Scoccimarro, E., Gualdi, S., Bellucci, A., Zampieri, M., and Navarra, A. (2016) Heavy
679 precipitation events over the Euro-Mediterranean region in a warmer climate: results from
680 CMIP5 models. *Reg Environ Change* 16: 595-602.

681 Shannon, P., Markiel, A., Ozier, O., Baliga, N.S., Wang, J.T., Ramage, D. et al. (2003)
682 Cytoscape: a software environment for integrated models of biomolecular interaction
683 networks. *Genome research* 13: 2498-2504.

684 Sommaruga, R., Hofer, J.S., Alonso-Sáez, L., and Gasol, J.M. (2005) Differential sunlight
685 sensitivity of picophytoplankton from surface Mediterranean coastal waters. *Appl Environ
686 Microbiol* 71: 2154-2157.

687 Steele, J.A., Countway, P.D., Xia, L., Vigil, P.D., Beman, J.M., Kim, D.Y. et al. (2011)
688 Marine bacterial, archaeal and protistan association networks reveal ecological linkages.
689 *ISME J* 5: 1414.

690 Stoeck, T., Bass, D., Nebel, M., Christen, R., Jones, M.D., BREINER, H.W., and Richards,
691 T.A. (2010) Multiple marker parallel tag environmental DNA sequencing reveals a highly
692 complex eukaryotic community in marine anoxic water. *Mol Ecol* 19: 21-31.

693 Teeling, H., Fuchs, B.M., Becher, D., Klockow, C., Gardebrecht, A., Bennke, C.M. et al.
694 (2012) Substrate-controlled succession of marine bacterioplankton populations induced by a
695 phytoplankton bloom. *Science* 336: 608-611.

696 Teeling, H., Fuchs, B.M., Bennke, C.M., Krueger, K., Chafee, M., Kappelmann, L. et al.
697 (2016) Recurring patterns in bacterioplankton dynamics during coastal spring algae blooms.
698 *Elife* 5: e11888.

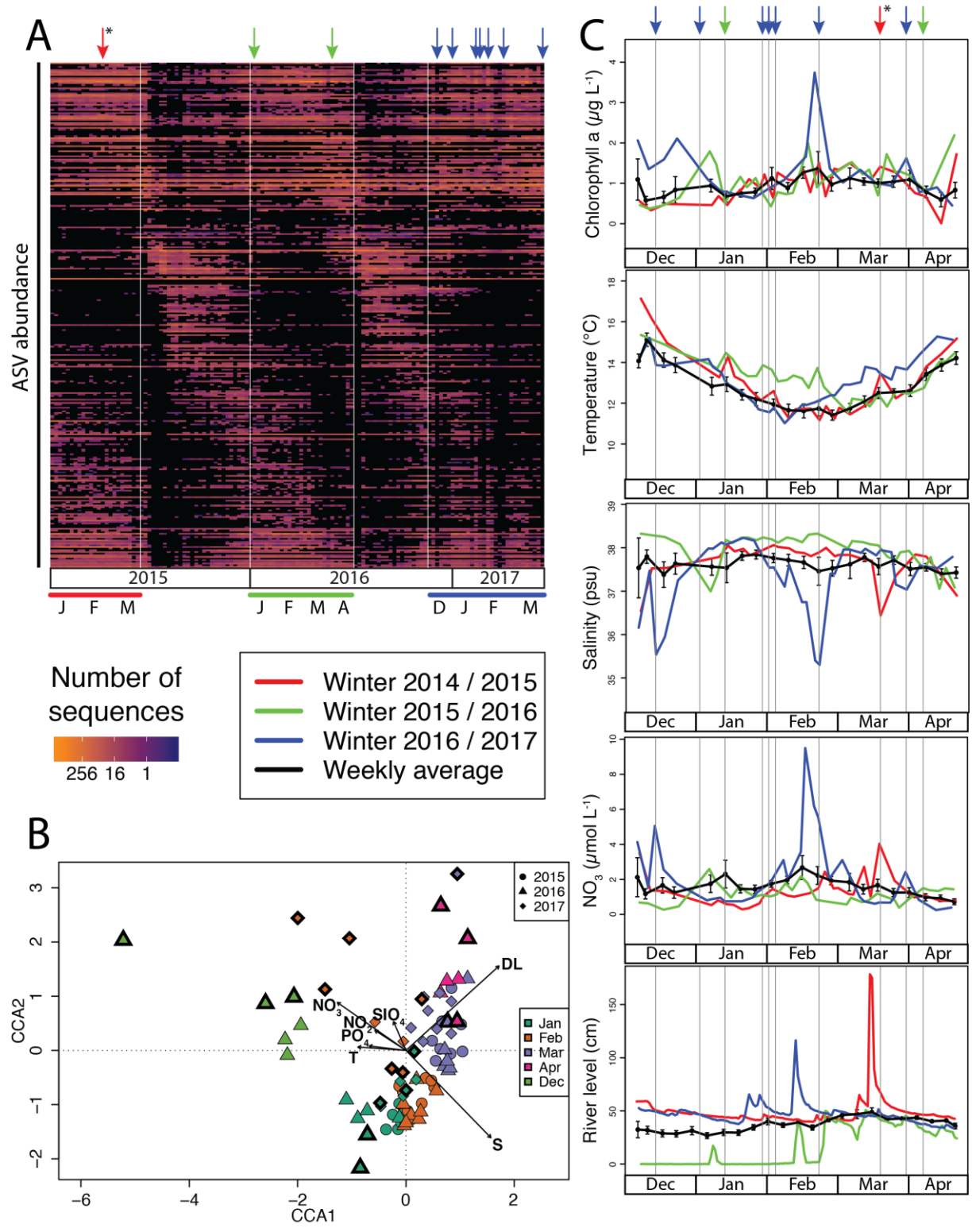
699 Thyssen, M., Grégori, G.J., Grisoni, J.-M., Pedrotti, M.L., Mousseau, L., Artigas, L.F. et al.
700 (2014) Onset of the spring bloom in the northwestern Mediterranean Sea: influence of
701 environmental pulse events on the in situ hourly-scale dynamics of the phytoplankton
702 community structure. *Front Microbiol* 5: 387.

703 Tinta, T., Vojvoda, J., Mozetič, P., Talaber, I., Vodopivec, M., Malfatti, F., and Turk, V.
704 (2015) Bacterial community shift is induced by dynamic environmental parameters in a
705 changing coastal ecosystem (northern Adriatic, northeastern Mediterranean Sea)—a 2-year
706 time-series study. *Environ Microbiol* 17: 3581-3596.

707 Treusch, A.H., Vergin, K.L., Finlay, L.A., Donatz, M.G., Burton, R.M., Carlson, C.A., and
708 Giovannoni, S.J. (2009) Seasonality and vertical structure of microbial communities in an
709 ocean gyre. *ISME J*.

710 Vellend, M. (2010) Conceptual synthesis in community ecology. *Q Rev Biol* 85: 183-206.

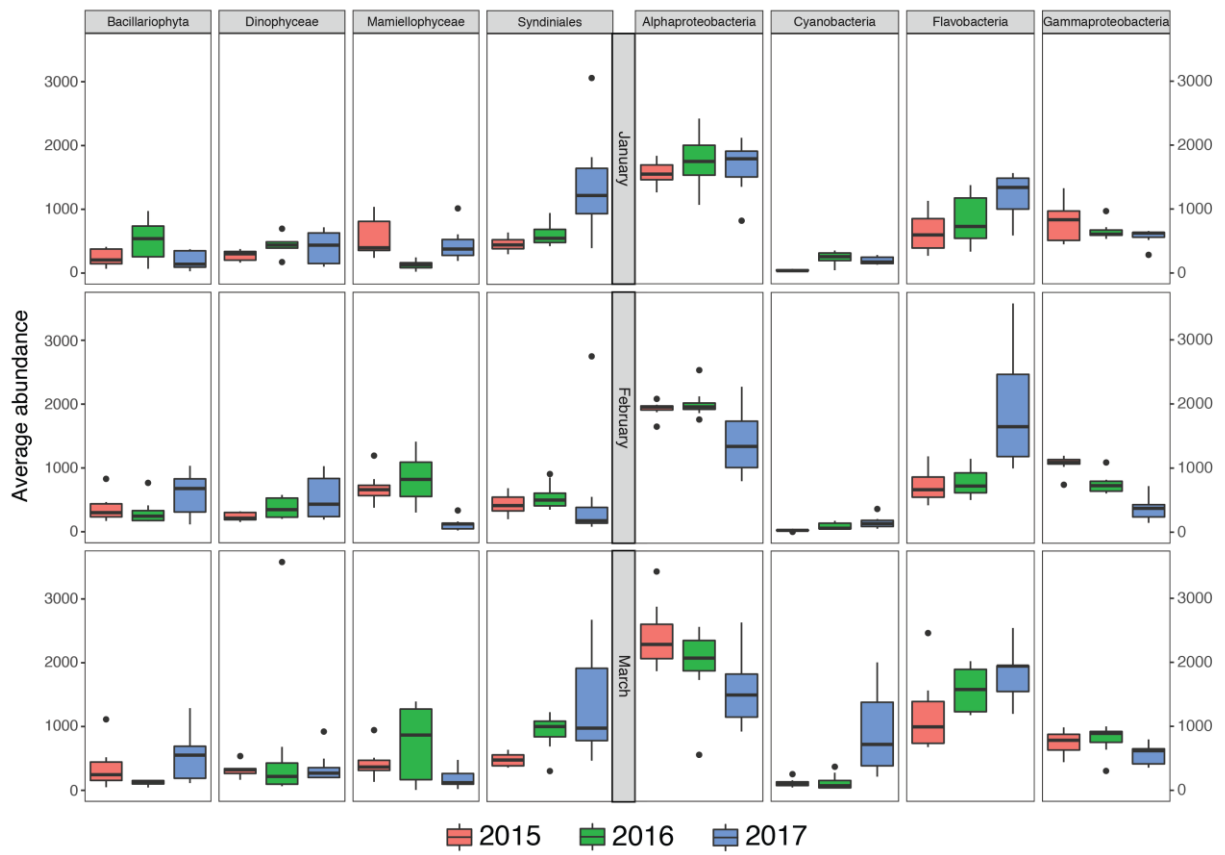
711 Wang, Q., Garrity, G.M., Tiedje, J.M., and Cole, J.R. (2007) Naive bayesian classifier for
712 rapid assignment of rRNA sequences into the new bacterial taxonomy. *Appl Environ*
713 *Microbiol* 73: 5261-5267.
714 Ward, C.S., Yung, C.-M., Davis, K.M., Blinebry, S.K., Williams, T.C., Johnson, Z.I., and
715 Hunt, D.E. (2017) Annual community patterns are driven by seasonal switching between
716 closely related marine bacteria. *ISME J* 11: 1412.
717
718
719
720
721
722
723
724
725
726
727
728
729
730
731
732
733



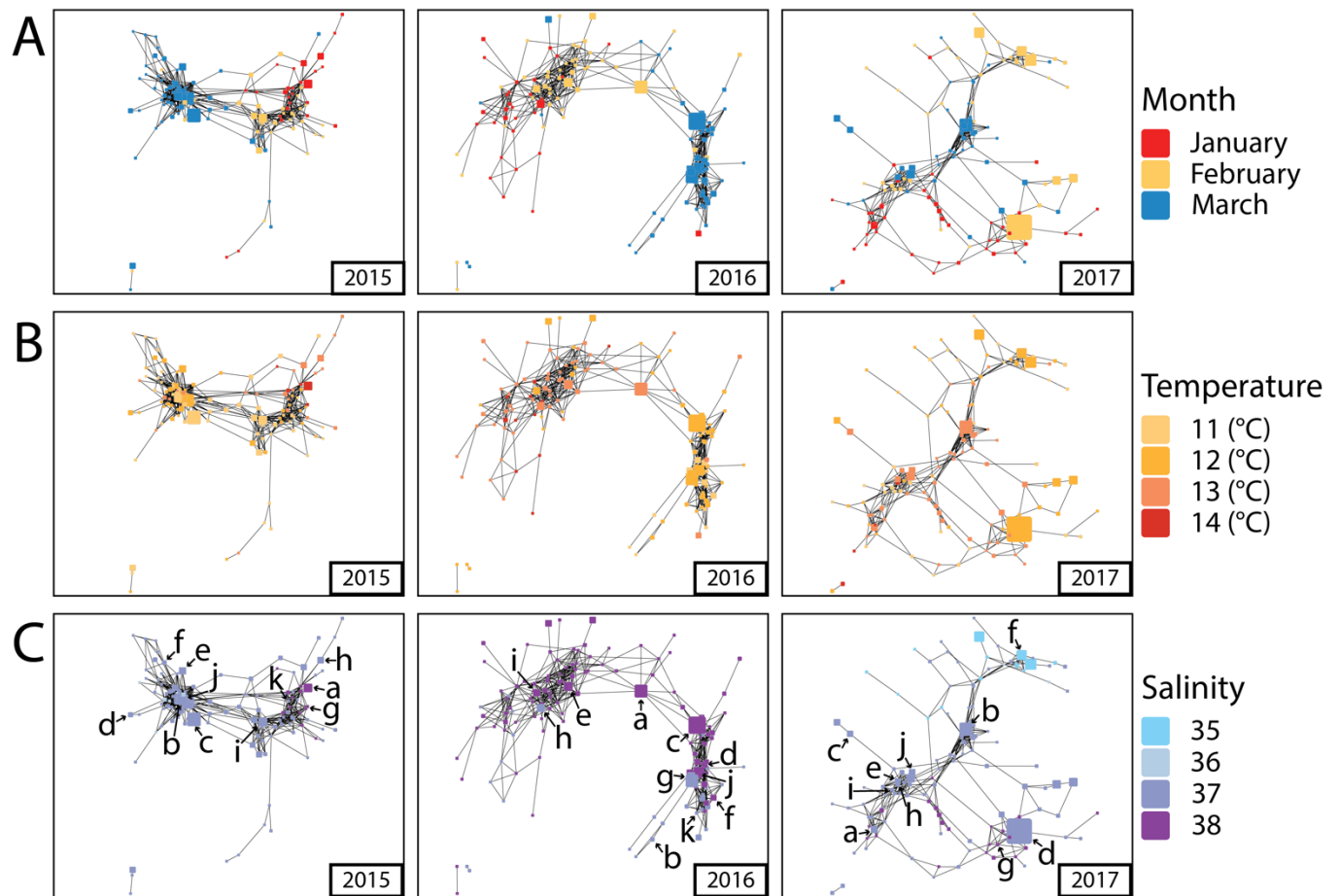
734
735
736
737
738
739
740
741
742

Fig. 1

743
744

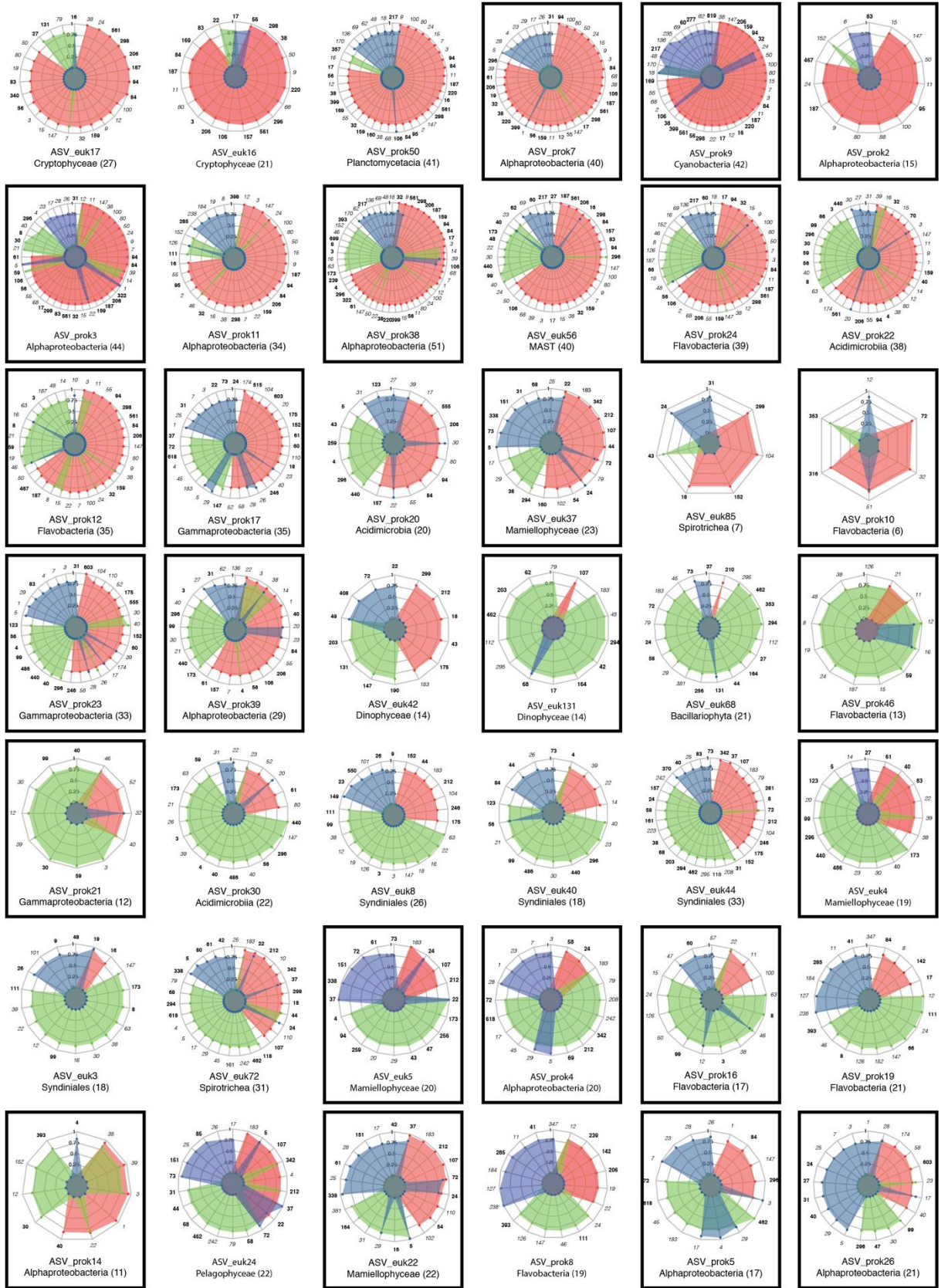


745
746 Fig 2
747
748



749
750
751

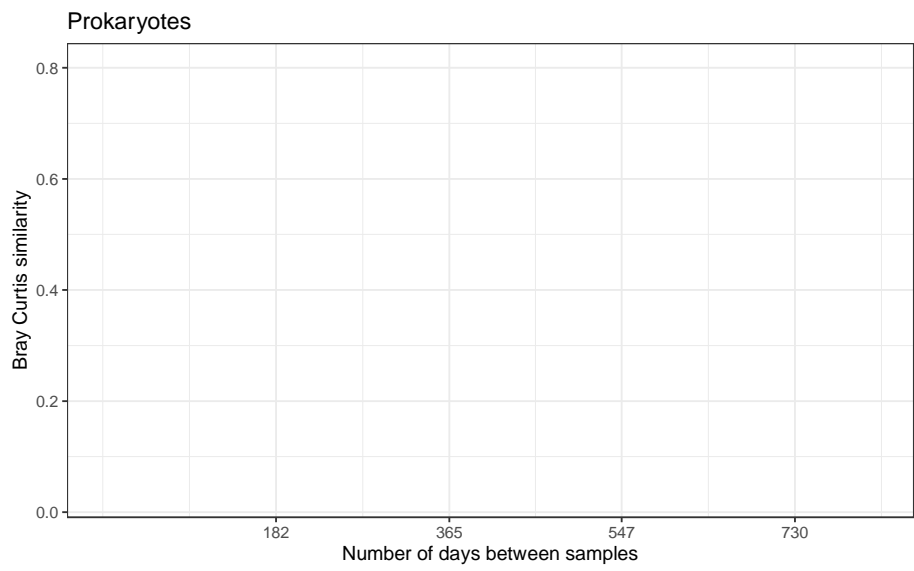
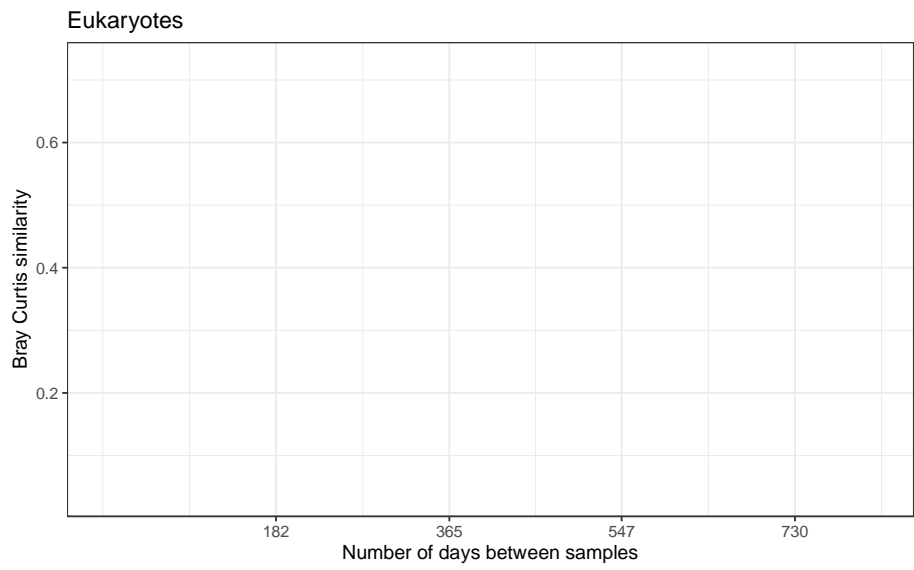
Fig 3



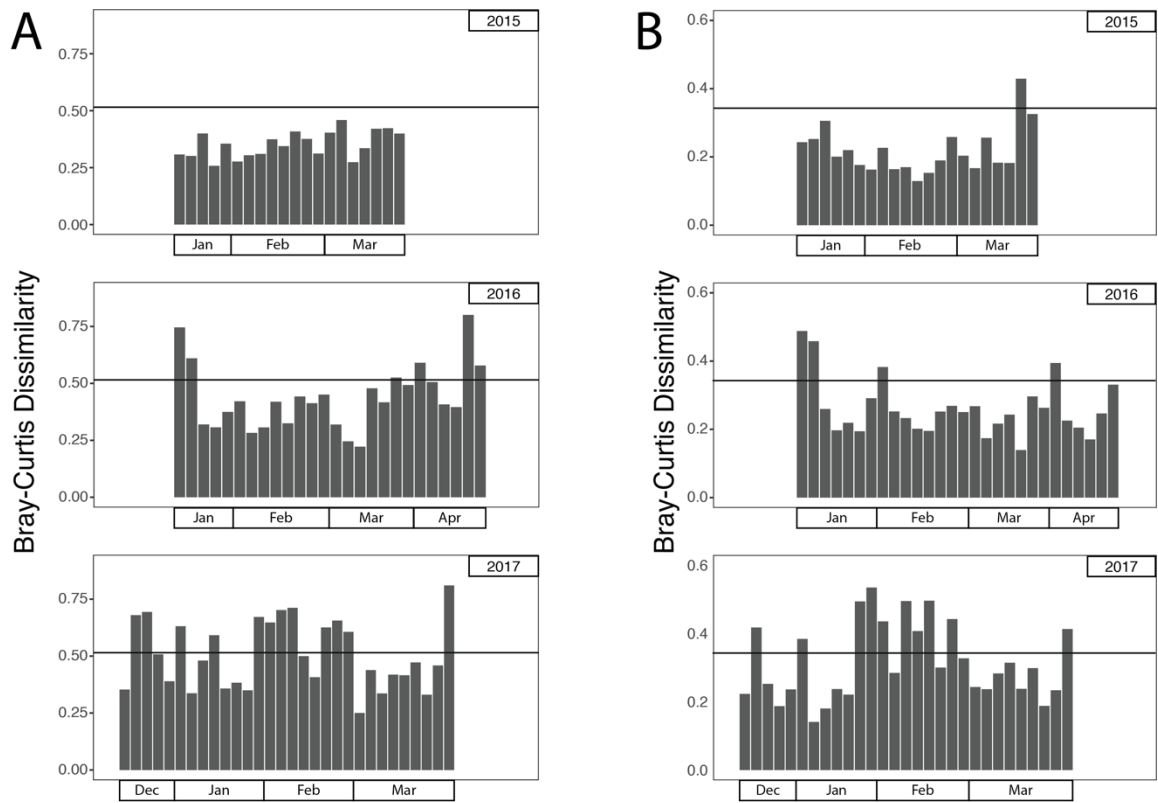
● 2015 ● 2016 ● 2017

752
753
754
755

Fig 4

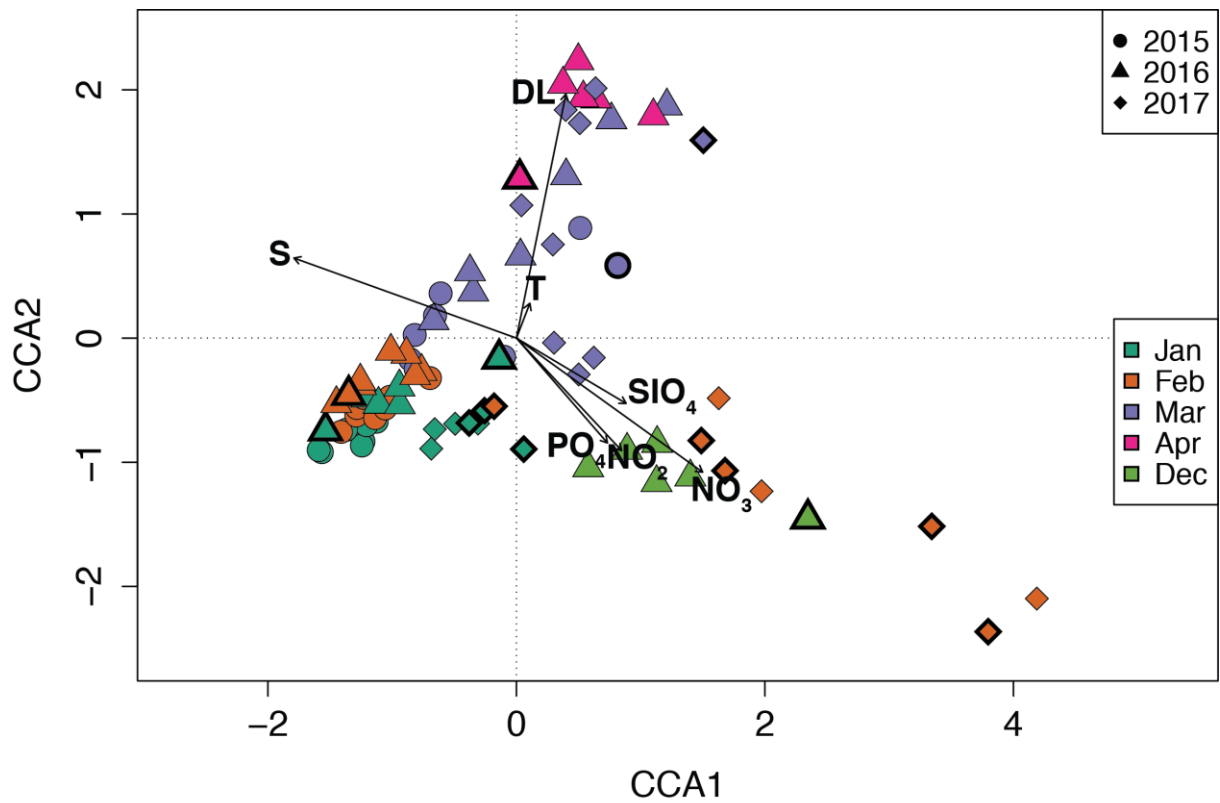


756
757 Supplementary Fig. 1



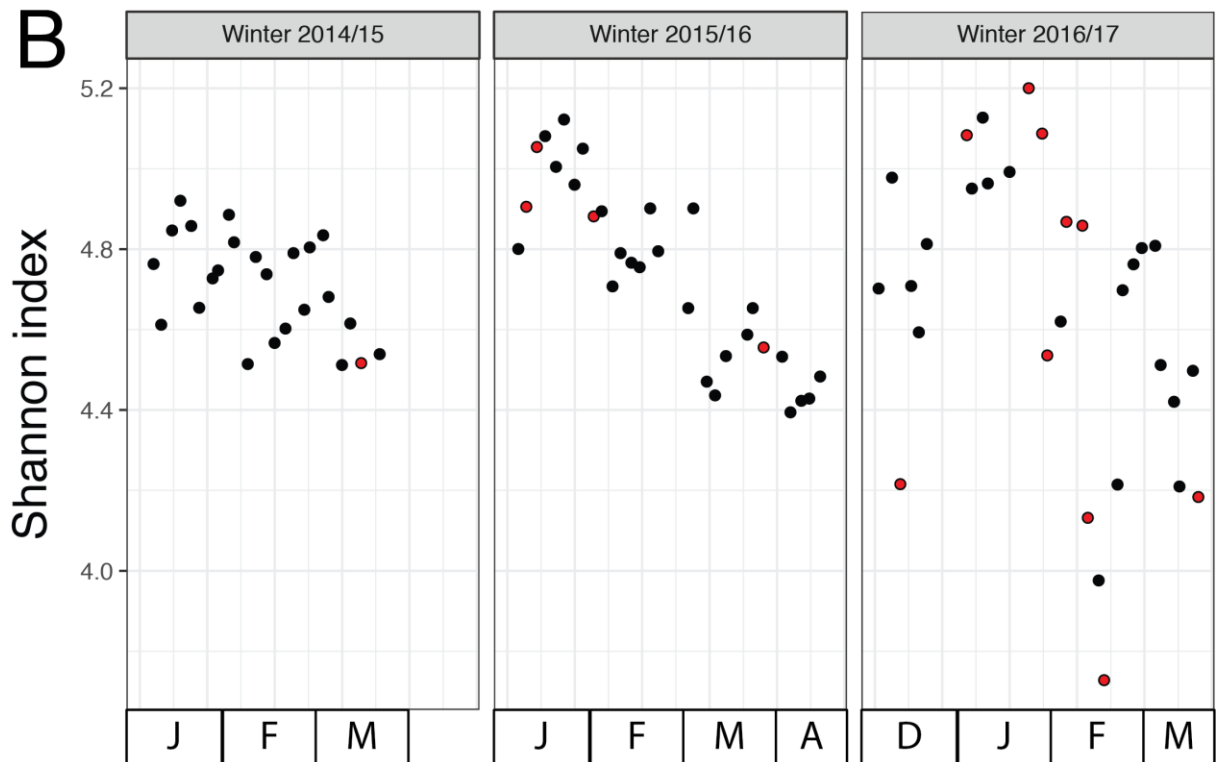
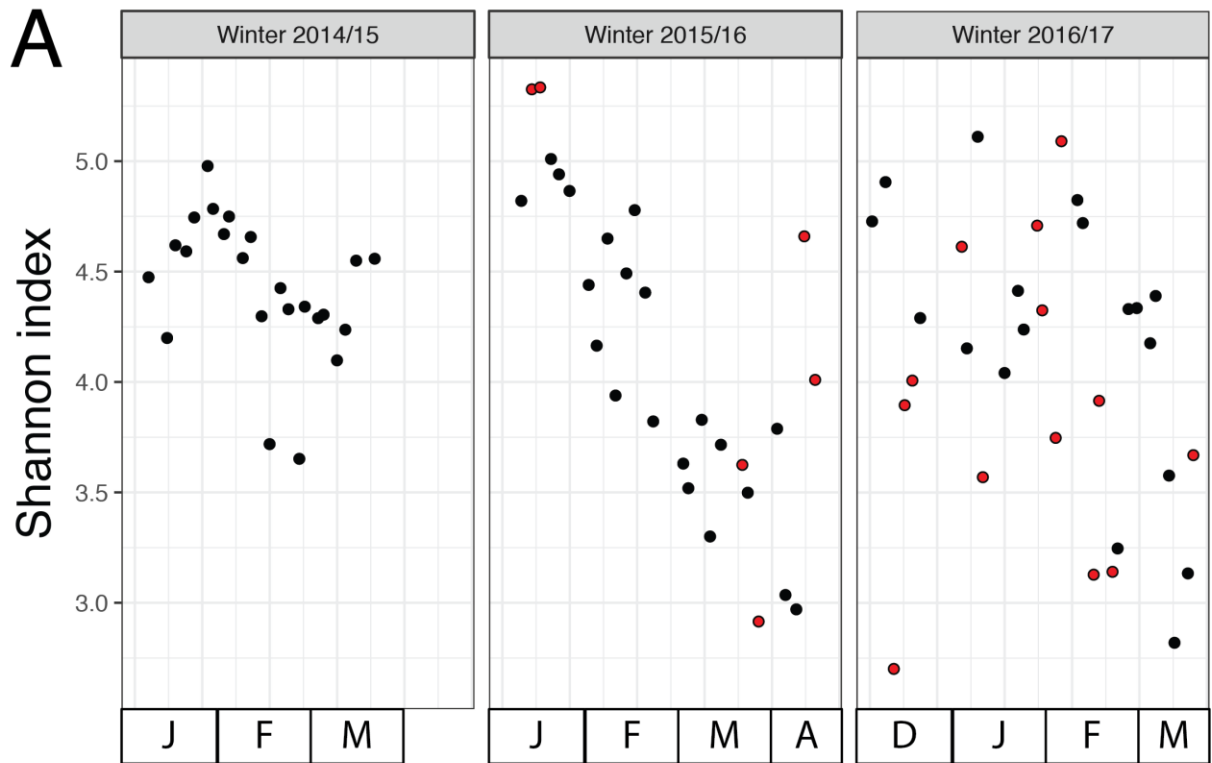
758
759
760
761

Supplementary Fig. 2



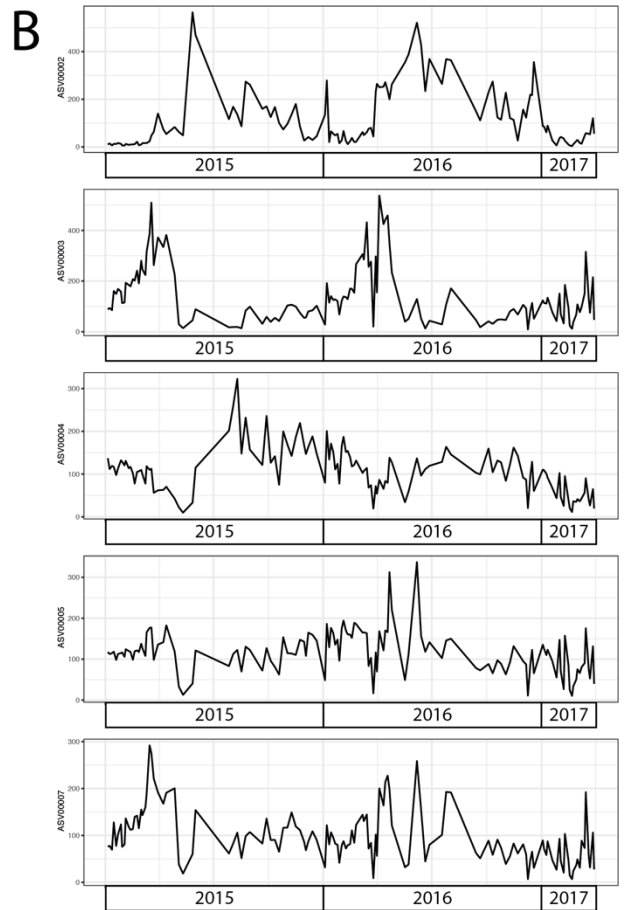
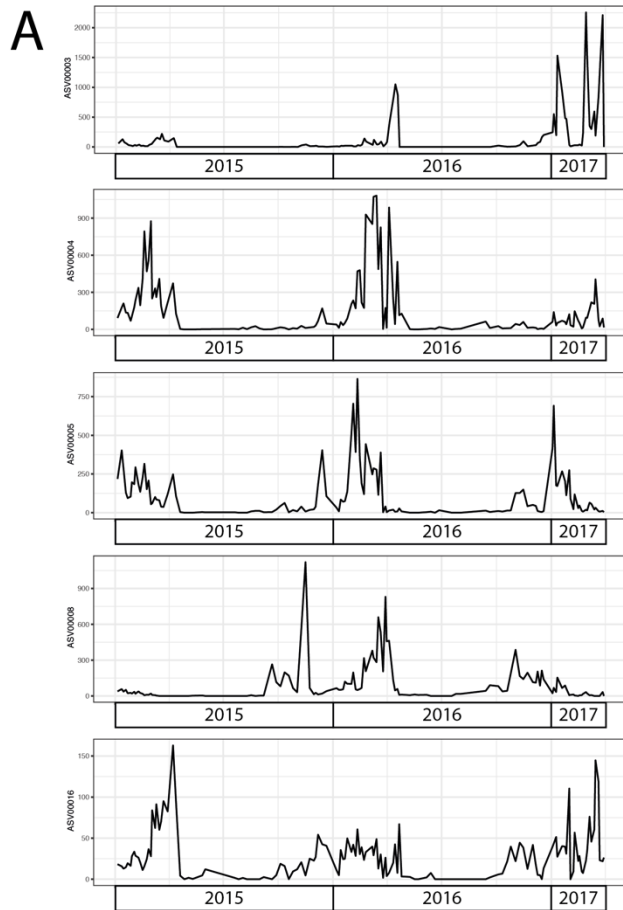
762
763
764
765

Supplementary Fig. 3



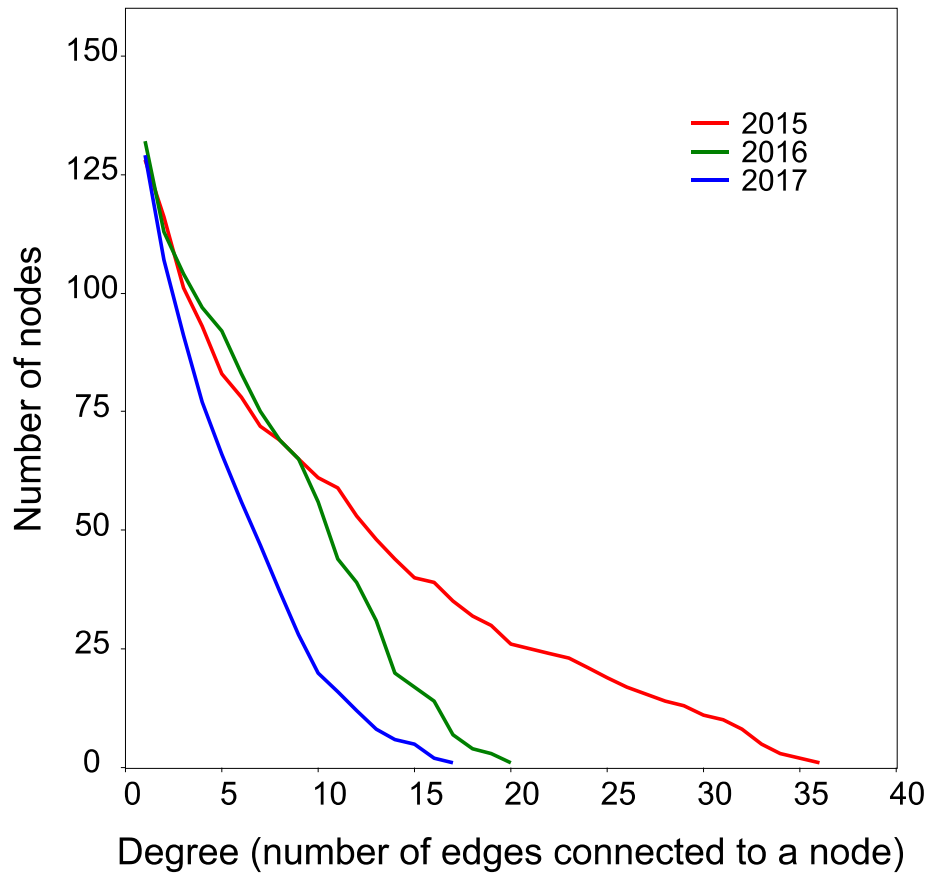
766
767

Supplementary Fig. 4

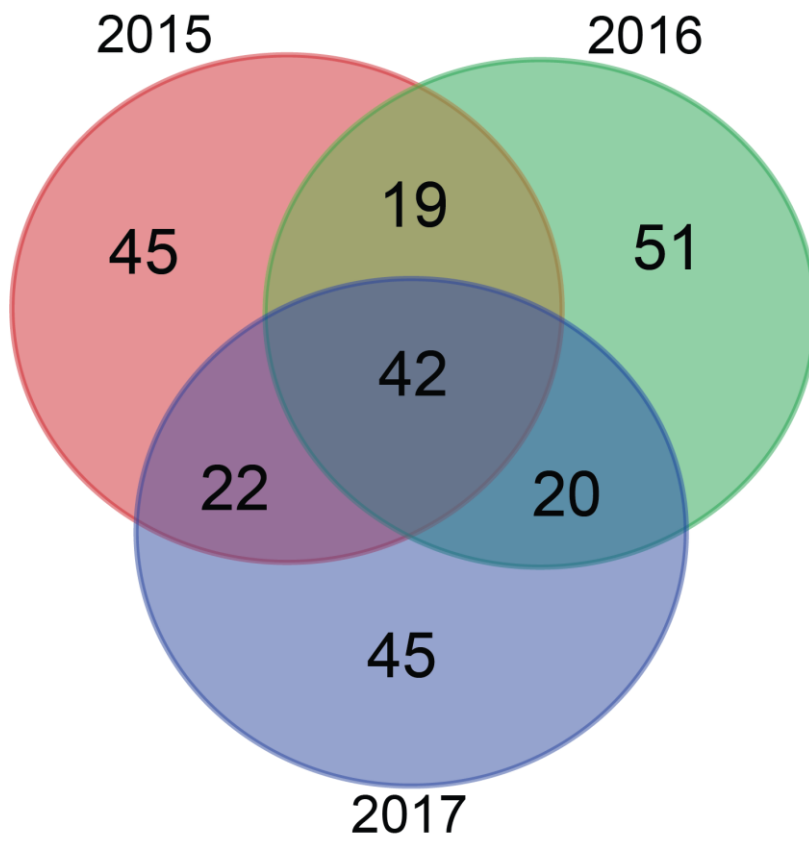


768
769
770
771
772

Supplementary Fig. 5



773
774 Supplementary Fig. 6
775
776



777
778
779
780
781
782
783
784
785
786
787
788
789
790
791
792
793
794
795
796
797
798
799
800
801
802

Supplementary Fig. 7